IEEE Photonics Journal
An IEEE Photonics Society Publication

Engineering Adiabaticity for Efficient Design of Photonic Lanterns

Volume 13, Number 2, April 2021

Sugeet Sunder
Anurag Sharma, ***Senior Member, IEEE***

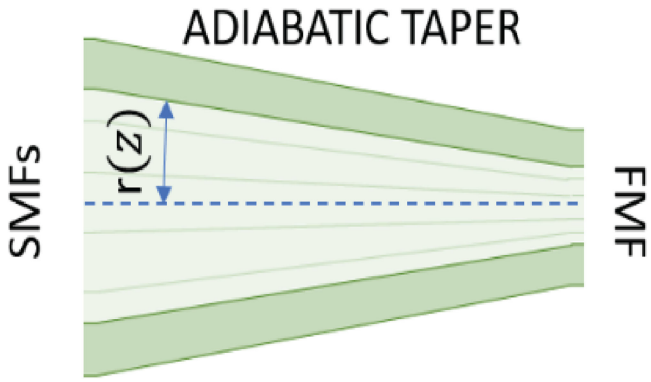

DOI: 10.1109/JPHOT.2021.3058361

IEEE photonics SOCIETY
IEEE

Engineering Adiabaticity for Efficient Design of Photonic Lanterns

Sugeet Sunder and Anurag Sharma, *Senior Member, IEEE*

Department of Physics, Indian Institute of Technology Delhi, New Delhi 110016, India

DOI:10.1109/JPHOT.2021.3058361

Manuscript received November 4, 2020; revised February 3, 2021; accepted February 7, 2021. Date of publication February 10, 2021; date of current version February 26, 2021. The work of Sugeet Sunder was financially supported by the University Grants Commission, Government of India. The work of Anurag Sharma was supported by the 'Class of 66' Chair Professorship and J.C. Bose Fellowship (SERB, Government of India). Corresponding author: Sugeet Sunder (e-mail: sugeet@physics.iitd.ac.in).

Abstract: We present a comprehensive systematic framework for optimizing adiabaticity in photonic lanterns. The framework considers the effects of both the cross-sectional and longitudinal device parameters on adiabaticity. Photonic lanterns are adiabatic photonic devices and are therefore known to have large device lengths. A Shortcuts-to-adiabaticity (STA) protocol is employed to optimize the adiabatic taper profile in all-fibre photonic lanterns. The method tailors adiabatic propagation of light in the system by appropriately correcting the local slope of the taper profile. A quantifiable measure of adiabaticity is established, based on the adiabaticity criterion. This measure relates inversely to the device length and is a useful parameter in taper optimization. We apply the protocol to reported photonic lantern devices to obtain optimal adiabatic taper profiles having shorter device lengths. The optimized taper profile refers to that taper profile which corresponds to the minimum local inter-modal coupling at every point along the quasi-adiabatic transition for a given device length. While optimizing the adiabatic transition by minimizing inter-modal coupling is the basic aim of this work, length optimization is an extremely useful by-product. This procedure can be used to either reduce the device length or to reduce the mode-coupling losses or both. This study analyses reported three and six-core mode selective photonic lanterns as examples. We also discuss ways to make the optimum profiles practically realizable.

Index Terms: Adiabatic coupler, photonic lantern.

1. Introduction

The adiabatic theorem was introduced in 1928 by Born and Fock [1], ever since it is extensively used to study controlled evolution in physical systems [2]–[4]. Adiabaticity is exploited heavily in areas like quantum control, quantum computation and other areas of quantum mechanics probably because it adds determinism and control to probabilistic systems [5], [6]. The wave-guiding structures in optics and photonics have found similarities to quantum systems, for example, a simple waveguide mimics a quantum well [7], [8]. Time evolution in quantum mechanics is analogous to electromagnetic propagation in optical systems. We may further extend the discussion by applying the ideas of adiabatic evolution to guided wave systems [9]. Adiabatic variations in guided wave systems are generally associated with tapering of the structures [10]. Tapering could be a reduction in the dimensions of the composite waveguide as a whole or the reduction of gaps between waveguides. The renewed interest in adiabaticity in the field of photonics is responsible

for the design of novel photonic devices like the Y-splitter, photonic lantern and other adiabatic converters [11]–[13].

Initially designed to solve an astro-photonic problem of OH suppression [14], the photonic lantern has come a long way. It is today considered as a useful tool in the solution of the imminent bandwidth issue [15]. Newer degrees of freedom like spatial and modal multiplicity have paved the way for Space Division Multiplexing (SDM) and Mode Division Multiplexing (MDM) which are envisaged as the plausible solutions for increasing the information-carrying capacity of optical network systems [16]. These emerging frontiers of SDM, MDM, and also the generation of orbital angular momentum modes in waveguides are some of the areas where photonic lantern devices have proved to be useful [17]–[20].

A photonic lantern is essentially a three-dimensional coupler having N single-mode fibres which are adiabatically tapered down to a few-mode fibre (FMF) with N modes. Though there are many methods of fabricating such devices, they can be realized by the adiabatic taper of a bunch of single-mode fibres within a low index capillary, in such a way that N such fibres are tapered together to a final multimode structure which can support N modes [21]. The working of the device and its salient features discussed in this paper will not be significantly affected by any specific fabrication technique. The study presenting the optimization of the taper profile is generic and independent of the different fabrication techniques for photonic lanterns.

Adiabaticity allows for a low loss transition from a known mode of a simple structure to a known mode of a more complicated structure [22]. An adiabatic transition must be sufficiently gradual, which usually means that the device length would be substantial. Defining the slowness criteria, also called the adiabaticity criterion, has been a subject of many papers [10], [23]–[25]. While this field is well developed in reference to quantum mechanics [26], [27] there have been significant contributions in extending the same to the context of photonic devices [10], [22]. A criterion for adiabaticity in fibre tapers was previously reported, where the maximum adiabatic taper angle is related to the beat length [10]. For the case where the system consists of two modes, the maximum taper angle for adiabaticity is defined as [10]

$$\Omega(z) = \frac{\rho(z)(\beta_1(z) - \beta_2(z))}{2\pi} \tag{1}$$

where $\beta_{1,2}(z)$ represent the propagation constants of the two modes and $\rho(z)$ denotes the radius of the inner cladding. While this angle is not a clear delineating criterion, it marks a length scale for the device. The actual angle must be far smaller compared to the maximum taper angle defined above. Extending the same to the multiplicity of modes, we categorize the modes into degenerate mode groups, and the maximum taper angle would then be dictated by the least beat length with respect to distinct mode groups at all points along the transition. This length scale criterion was further improved considering the effects of the mode profile, the effective index and other waveguide parameters for special cases [28], [29].

The adiabatic theorem mathematically defines the slowness in terms of the eigenvalues and eigenfunctions [30]. In the context of photonic devices, this may be written as

$$\left| \frac{\langle a | \dot{b} \rangle}{(\beta_a - \beta_b)} \right| \ll 1 \tag{2}$$

where the dot denotes derivative with respect to the propagation distance z and $\beta_{a,b}$ are the propagation constants associated with the modes $|a\rangle$ and $|b\rangle$ of the transverse cross-sectional refractive index profile, respectively. A controlled evolution of the field could be achieved by forcing a slow variation of the modes along the propagation direction. Consequently, the length of the device is large in adiabatic devices, analogous to large time scales in adiabatic quantum processes. Adiabatic devices, in turn, tend to be robust in terms of broadband operations and contribute towards good fabrication tolerances [30]. Optimization of this trade-off between large device lengths and adiabatic control has led to the development of a class of techniques used to accelerate the adiabatic process optimally, called Shortcuts-To-Adiabaticity (STA) [31]. One of the

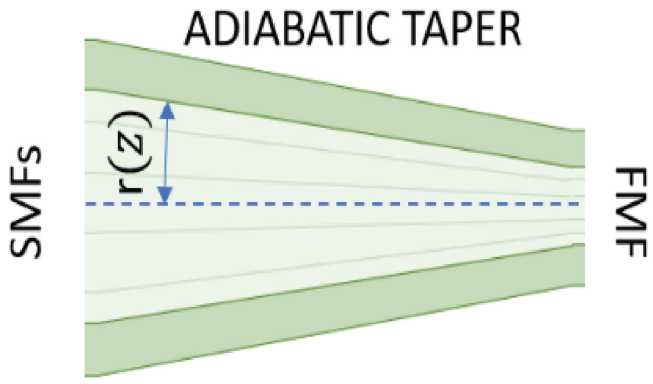

Fig. 1. Schematic of a photonic lantern.

STA protocols, fast quasi-adiabatic dynamics (FAQUAD) was applied successfully to an asymmetric Y-junction mode sorter [30]. Using a similar analysis, we present a method to optimize the photonic lantern device length by tailoring adiabaticity. The next section outlines the protocol. Further, we demonstrate its application on structures that have been well analysed and reported in literature. The effect of the measure of quasi-adiabaticity on the propagation and retention of power in a certain mode has also been discussed.

2. Optimization Protocol

This protocol is applicable to systems with a single adiabaticity control parameter. The control parameter could be the gap between components of the device, the radius of a certain waveguide or as in our case the dimension of the composite structure. A photonic lantern merely tapers along the propagation direction; hence, its adiabatic evolution is governed by a single control parameter defining the transverse size. The optimization protocol homogenizes adiabaticity over the adiabatic evolution. The measure of adiabaticity is indicative of the measure of coupling between modes. This measure varies along the transition and can be defined for a two mode system as [30]

$$\left| \frac{\langle a| \frac{\partial}{\partial z} |b\rangle}{(\beta_a - \beta_b)} \right| = \varepsilon(z) \tag{3}$$

where $\varepsilon(z)$ represents the magnitude of mode coupling along the propagation axis. Since, the entire structures tapers uniformly, it suffices to consider one parameter as a control parameter. In the case of photonic lanterns, as shown schematically in Fig. 1, we consider the radius of the inner cladding $r(z)$ as this parameter. As the structure tapers, this parameter assumes the role of the radius of the core at the tapered FMF end. We, can now rewrite eqn.(3) as

$$\left| \frac{dr}{dz} \frac{\langle a| \frac{\partial}{\partial r} |b\rangle}{(\beta_a - \beta_b)} \right| = \varepsilon(z) \tag{4}$$

The term in the left hand side (LHS) of eqn.(4) can be considered as a product of two factors, where we immediately observe that the second factor depends only on r. The first factor in this product term gives the relation between r and z; $r(z)$ thus defines the taper profile. We may now define the second factor on the LHS which is a function of r alone, as

$$G(r) = \left| \frac{\langle a| \frac{\partial}{\partial r} |b\rangle}{(\beta_a - \beta_b)} \right| \tag{5}$$

The structure tapers along the propagation direction and $r(z)$ can be safely considered to be monotonically decreasing, i.e., it has the same sign throughout. Therefore, we may now write

eqn.(4) as

$$-G(r)\frac{dr}{dz} = \varepsilon(z) \tag{6}$$

Here, $G(r)$ and $\varepsilon(z)$ represent measures of mode coupling as a function of r and z respectively, while $r(z)$ denotes the taper profile. For a given profile, $G(r)$ would have an implicit dependence on z through $r(z)$. However, $G(r)$ does not depend on the profile $r(z)$ as it is a function of r alone. It depends on the characteristics of the two modes and their variation as a function of r. Thus $G(r)$ remains unchanged if the profile $r(z)$ between two given values of r is changed. On the other hand $\varepsilon(z)$ would certainly change if $r(z)$ is changed. This relation is governed by eqn.(6).

Let the taper be such that r changes from r_1 to r_2 over a length L. We may integrate eqn.(6) to get

$$\int_{r_1}^{r_2} -G(r)dr = \int_0^L \varepsilon(z)dz \tag{7}$$

For a given two-mode system on any arbitrary monotonically reducing taper profile $r(z)$ between r_1 and r_2, the LHS is constant. Thus,

$$\int_0^L \varepsilon(z)dz = constant \tag{8}$$

This shows that irrespective of the taper profile, the area under the $\varepsilon(z)$ curve would remain unchanged for a given modal system, between r_1 and r_2. Therefore, for a desired variation of $\varepsilon(z)$ we can solve eqn.(6) to obtain a corresponding $r(z)$. For a transition to be adiabatic or strictly quasi-adiabatic, we must have $|\varepsilon(z)| << 1$. Since, the area under $\varepsilon(z)$ is a constant [eqn.(8)], the best case would be when $\varepsilon(z)$ has a constant of value much less than 1, as a lower value of $\varepsilon(z)$ would necessarily require a higher value at some other z to keep the area under the curve $\varepsilon(z)$ constant. This immediately gives a relation between the length of the device, L, and the constant value ε_c.

$$\varepsilon_c = \frac{1}{L}\int_{r_1}^{r_2} -G(r)dr \tag{9}$$

Thus, for a given modal system with r_1 and r_2 as limiting sizes, one may choose a large value of L to keep ε_c sufficiently small. For any chosen value of L one can obtain the value of ε_c and the corresponding optimal taper profile $r(z)$ by solving eqn.(6). However, the extent of quasi-adiabaticity of the profile would be dictated by the value of ε_c.

This protocol can be directly extended to systems with more than two modes. In this study, we have considered photonic lanterns systems with a multiplicity of modes and degeneracy in some modes. For an N core photonic lantern, the calculation of $G(r)$ becomes, $G(r) = max[G_{ij}]i,\ j(\neq i)$ refer to modes or mode groups in case of degeneracy and G_{ij} is the value of $G(r)$ between the i^{th} and the j^{th} mode/mode groups. In a sense, for every value of r we are trying to find the pair of modes where the coupling or the damage to adiabaticity is maximum. Therefore, all other mode pairs are more quasi-adiabatic than that pair at that specific position. Thus, the variation $G(r)$ contains the worst case of quasi-adiabaticity, implying that satisfying the same would automatically take care of the other mode pairs at that value of r. Using this $G(r)$, we then obtain at the most appropriate variation $r(z)$ for chosen values of ε_c and L. The computed optimal variation of $r(z)$ could further be fitted to a polynomial or a known function to obtain a smoother functional form. This fitting would, however, be such that the fitted curve is always slightly more or equal to the actual $G(r)$, so that the obtained values of $G(r)$ for any value of r represent a case which is slightly less adiabatic. This would result in a taper profile which would have better adiabaticity than that dictated by the actual $G(r)$.

In this study, a five-point central difference scheme was used for calculation of the numerical derivative. The $G(r)$ thus obtained was fit to a certain functional form with respect to r. This fit would differ from case to case and for ease of calculation a small overestimation wherever necessary of its value at various r would help achieve a smoother and easy to compute quasi-adiabatic profile. The

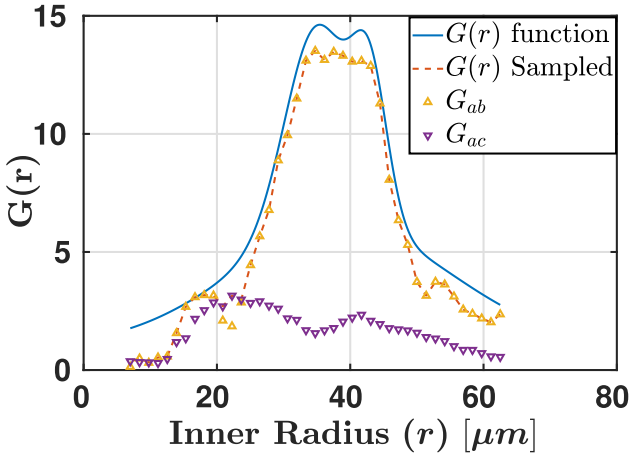

Fig. 2. Measure of coupling in units of the linear slope.

resulting profile obtained using the described method may not be easy for fabrication, especially on a conventional taper rig. We will address this issue in sec.4.

3. Three and Six Core Photonic Lantern

We demonstrate the applicability of the protocol described above in the context of photonic lantern devices. The protocol has been used to optimize the taper profile by reducing the device length while improving or maintaining adiabaticity. To this end, we have considered two different mode selective photonic lanterns, with three and six cores, respectively.

3.1 Three Core Photonic Lantern

We consider a three core photonic lantern, previously reported in [32] and also analyzed by [33], [34] with a device length of 20 mm. In general, the length of the photonic lantern scales quadratically with the number of cores [35]. The three-core device consists of 3 SMFs arranged as vertices of an equilateral triangle; the core diameters at the SMF end are 11, 8.8 and 7 microns which selectively excite LP_{01}, LP_{11a} and LP_{11b} modes of the delivery FMF end, respectively. An untapered 125 microns inner cladding tapers linearly into a 14 μm core which supports exactly three modes at a wavelength of 1.55μm. The structure has two mode groups, the fundamental mode $\{a\}$ and a degenerate pair $\{b, c\}$ of the first higher-order mode. The measure of adiabaticity for this system could be computed as $G(r) = max[G_{ab}(r), G_{ac}(r)]$, the sampled data points are then fitted to a well-behaved function by overestimating the values wherever required as discussed in the previous section. The evaluation of the function $G(r)$ at a sampled point requires the computation of the modal fields and the propagation constants at that sampled value of r. The modal field profiles $|a\rangle$, $|b\rangle$ and the respective propagation constants β_a and β_b may be computed using any standard method like finite element method [36], finite difference method [37] etc. However, we have used the collocation method, in which we convert the Helmholtz equation into an eigenvalue equation using a semi-analytical formalism. This method was also used in our earlier work and more details are given in [33]. The sampled $G(r)$ for different mode pairs, net sampled $G(r)$ and a three-Gaussian functional fit of $G(r)$ are plotted in Fig. 2.

It can be observed that the curve $G(r)$ has low values initially, increases with taper, and finally reduces again towards the end. This can be understood by observing that initially the individual cores of the SMFs are far apart making coupling very weak, but as the system tapers, the cores begin to interact and the device as a whole transitions to circular symmetry. The cores begin to loose their individual identity and the super-modes reshape themselves into orthogonal modes of

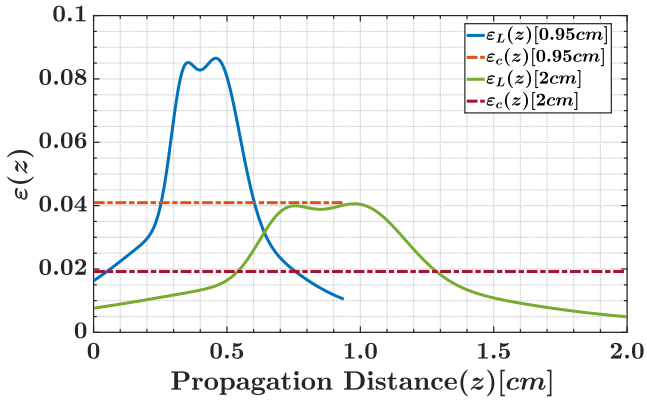

Fig. 3. Measure of adiabaticity for linear and optimized taper. The area under the curve is same for all the $\varepsilon(z)$ variations. The measure of adiabaticity for the reduced length in the optimized case $\varepsilon_{opt}(z)[0.95cm]$ is nearly equal to the most lossy value of $\varepsilon(z)$ in the linearly tapered device.

the FMF. After this transition, the value of coupling reduces again. Using equation (8), we compute the integral constant representing the area under $\varepsilon(z)$.

In Fig. 3 the area under the curves of optimized ε_c and ε_L (ε for a conventional linearly tapered device) for the lengths of 2 cm and 0.95 cm are same, since these correspond to the same fiber system and the area under the $G(r)$ curve as defined in eqn(7) remains the same. The figure shows that for the same length of 2 cm, an optimized taper profile would give a lower ε_c value resulting in less mode coupling and better mode purity. However, it can also been seen that for a relaxed tolerance on the acceptable values of $\varepsilon(z)$, as the variation of a practical linear taper design suggests ($\varepsilon_L(z)[2cm]$), an optimized taper of nearly half the device length (with $\varepsilon_c(z)[0.95cm]$) can be designed.

In order to compute the optimum taper profile, we first fix the required device length and the acceptable value of ε_c using this relation in equation (9). The relation suggests that ε_c and L vary inversely, implying that a shorter device length would compromise adiabatic propagation and increase coupling losses. After having fixed the desired length and having obtained the constant homogenized measure of coupling ε_c, it is but left to solve the differential equation (6) under the boundary conditions governing the value of inner radius $r(z=0) = 62.5\mu$m for the three-core structure. The obtained optimized variation of $r(z)$ for less than half the linear device length for the three-core device is plotted in Fig. 4. The optimized variation though mathematically accurate may not immediately seem suitable for fabrication. Thus, a procedure to obtain more practically realisable variations for $r(z)$ is outlined in the next section.

Taper optimization is primarily focused on reducing the power loss due to inter-modal coupling during propagation, thus maintaining modal purity. A study on the difference in fractional power retention by the fundamental mode and the first higher order mode during propagation in a linearly tapered device in comparison to the same through a device with optimized taper is plotted in Fig. 5. The plot shows the total power lost within the computational window as a function of propagation distance. The computational window is truncated by a layer of a gradually absorbing boundary, the specifications of which are indicated below.

It was observed that the power retention is much better in the optimized case compared to the case of linear taper of the same length. For both the modes, the fractional loss is less than half in the optimized device compared to the linear taper device. The graph in Fig. 5 cannot be directly juxtaposed and compared with Fig. 2, because the energy that is absorbed into the gABC layer which in effect is the energy lost out of the device, reaches the boundary layer only after a considerable propagation distance. Therefore, it is in a sense a delayed response, between the power coupled out at a certain point along the propagation and the plot in Fig. 5. The study clearly emphasises the importance of taper optimization for adiabatic propagation and optimum

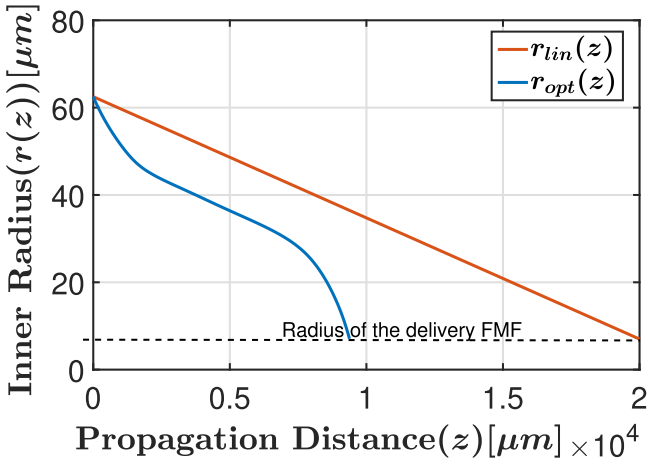

Fig. 4. Computed optimized quasi-adiabatic profile of the inner radius for a much shorter device length compared to linear taper profile.

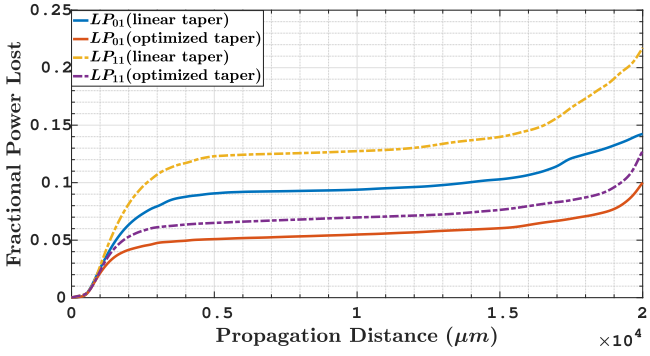

Fig. 5. The taper profile effects the fractional power retention in the device. The optimized taper shows a reduction of more than 50% in the power lost during propagation for both the distinct modes in the three-core device.

power retention. The total coupling loss is largely determined by the loss at most lossy point along the taper transition. Therefore, a uniformly quasi-adiabatic transition provides a robust check on this loss all along the transition. The reduction in length is also a useful by-product of the optimization process as discussed above. Other ways to reduce the taper length in linear devices is by considering graded-index SMFs. We have analyzed such devices and have found that these devices have a better $G(r)$ variation, thus allowing for more efficient devices at shorter device lengths. This aspect has been illustrated further for the case of six-core photonic lanterns later.

The simulation was performed using the a collocation method based beam propagation scheme [38] where the iterations are computed using the fourth-order Runge-Kutta method. The step size for numerical propagation was taken as 0.04μm, since the propagation is unaffected by further reduction in the step size. A gradually absorbing boundary condition (gABC) was implemented, which has been shown to be comparable to PML [39]. The gABC strength for a width of 40% was taken to be 0.89 with a sin^2 profile [39]. The gABC parameters are optimized and its effect on the propagation can be considered to be similar for both the cases.

3.2 Six Core Photonic Lantern

A variety of six-core photonic lanterns have reportedly been analysed in literature [40], [41], [42]–[44]. Variations being with geometries of circular [42] and elliptical core [43] and index distributions like graded [44] and step [41]. In tapering photonic lanterns with elliptical cores, such as the

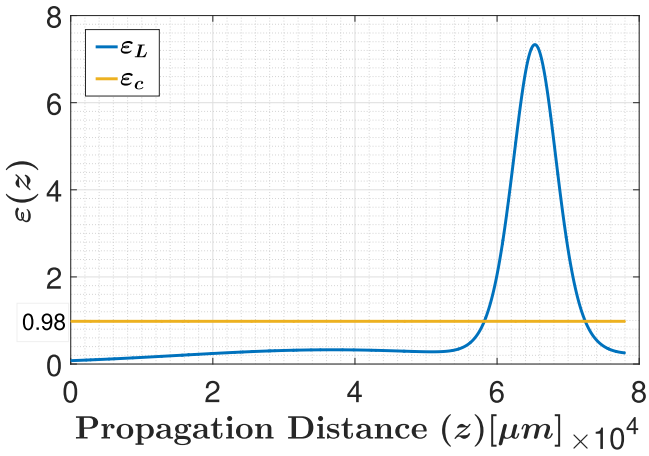

Fig. 6. The measure of coupling for the six-core photonic lantern. For the conventional case it is eight times higher than that with the optimized case for a 10% reduction in device length.

EC-MSPL described in [43], the ellipticity is maintained as both the major and minor axes taper proportionately. In such a case, the length of either axis maybe considered as the control parameter. The method is thus generic and can be applied to the elliptical core photonic lantern as well. However, in this work, we have considered the circular core mode selective photonic lanterns. Here, we have analysed, step index profiles reported in [33], [40], [43]. The six-core device has a low index capillary initially with a diameter of 280 microns. The six SMF cores that map onto six modes LP_{01}, LP_{11a}, LP_{11b}, LP_{21a}, LP_{21b}, LP_{02} of the FMF have diameters of 17μm, 15μm, 14μm, 13μm, 12.4μm and 10μm, respectively. An inner cladding of undoped silica is considered, while the outer cladding is considered to be fluorine doped with an index difference of -6×10^{-3} at a wavelength of 1.55μm. The doped SMF cores have a higher index of 1.45. Such structures work as MIMO free devices [45], [46] because of the one to one correspondence between an input individual SMF mode and a super-mode of the tapered structure. The structure has six modes over four mode groups. We may label them as a to f, with a and f corresponding to the LP_{01} mode and LP_{02} mode respectively. The degenerate pairs addressed as $\{b, c\}$ and $\{d, e\}$. The measure of coupling for this system could be computed as $G(r) = max[G_{ij}]$, where $i, j(\neq i) = a, b, c, d, e, f$. The same is then substituted in eqn.(6) to compute $\varepsilon(z)$. For, this structure, the curve of $\varepsilon_L(z)$ in Fig. 6 shows that initially at the untapered end, the coupling is very low. As discussed earlier, this is due to the SMF modes being well guided in the respective cores which are well separated from each other. As the structure tapers, the modes spread out of the high index cores and begin to interact. The modes of the system slowly move out of the individual core and evolve into the orthogonal modes of the composite structure with the inner cladding taking the role as the new wave-guiding core. Homogenization of $\varepsilon(z)$ would require to contain the slope of $r(z)$ in such a way as to compensate for the high values of $G(r)$.

The optimized $r(z)$ for the six-core case with a slight reduction (10%) in the device length is shown in Fig. 7. The value of integral in equation (9) limits the quasi-adiabatic device length in this system. While the reduction in the device length is not significant, the adiabaticity in the system is homogenized and the coupling is contained considerably along the entire length of the device. The discussion on six-core structures presented in [42] indicate that the adiabaticity of the device is not optimal and improves with a graded index profile. Similarly, in [43] the authors argue that an elliptical design reduces the modal cross-talk in the device, which in essence improves the adiabaticity. We note that the device under a linear taper transition is inherently not very adiabatic. While the linear device does provide the expected I/O characteristics, it is intuitive that a homogeneously adiabatic profile provides greater control and robustness to the device under the adiabatic transition. The fabrication of such complex taper profiles may seem unreasonable, however, we could approximate the optimized profile with a suitable smooth function that can be fabricated with relative ease.

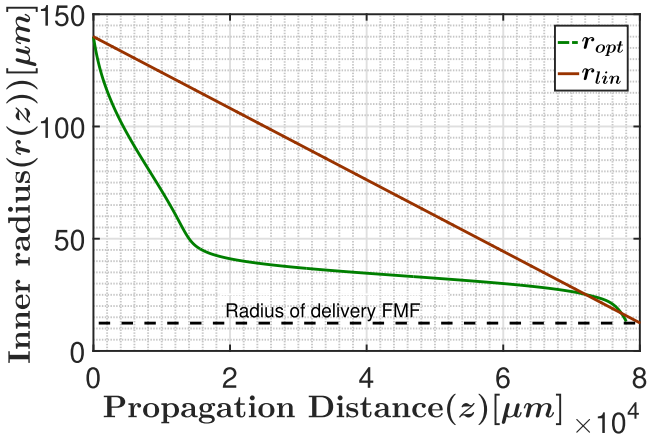

Fig. 7. The slope of $r(z)$ in the optimal taper ensures that the coupling is minimal at every position along the transition.

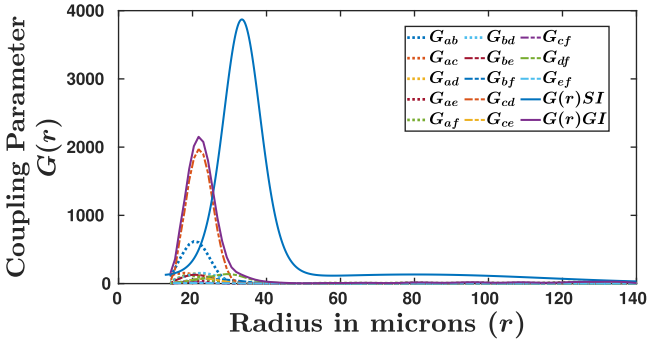

Fig. 8. Effect of a graded index profile on the coupling parameter. Here *a*, *b*, *c*, *d*, *e*, and *f* refer to LP_{01}, LP_{11a}, LP_{11b}, LP_{21a}, LP_{21b} and LP_{02} respectively.

Intuitively, a linear profile may seem to be optimal because the slope at any point is constant, in the case of any other profile, a slowly varying non-linear part at any point will be compensated by a rapidly varying part which could compromise adiabaticity. The argument is since the slope at each point represents the rate of taper; thus, a faster rate of taper would imply more coupling. However, this clearly is not the case. The measure of adiabaticity, at any point along the taper is dependent not just on the slope of taper, but also on the mode coupling characteristics which in turn depend on the cross-sectional index distribution, field profiles and propagation constants.

3.3 Graded Index SMFs

It has been shown that graded index SMFs can be used to obtain shorter device lengths in photonic lanterns [42]. The authors have shown a reduction in device length by a factor of 2, mode purities were shown to be preserved at 4 cm[42]. The effect of the same can be observed in the analysis of adiabaticity in such structures. We performed the STA analysis as discussed above on the graded index profile to understand the effect of using graded index SMFs. The graded index fibers based PL also has six cores and supports four mode groups of LP_{01}, LP_{11}, LP_{21} and LP_{02}. The core indices used in this case are same as the case of the step index fiber based PL discussed above and a parabolic-index profile has been considered. Variations of $G(r)$ for different mode pairs and the final variation of $G(r)$ for a graded-index six-core case have been plotted in the Fig. 8. It has been compared with the step-index profile discussed above. It can be seen that the maximum value of

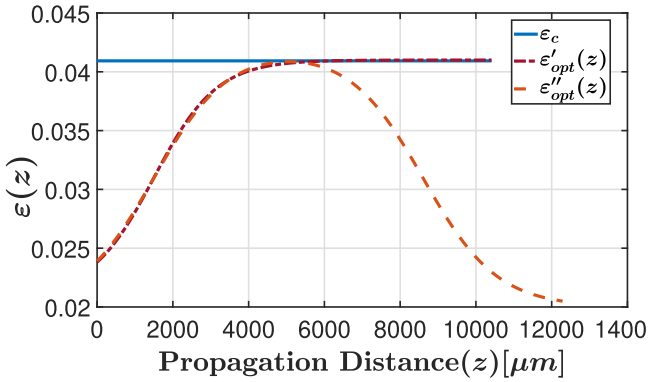

Fig. 9. Tailoring of the $\varepsilon(z)$ for the optimized taper profile to reduce the profile slopes at the two extreme ends.

$G(r)$ (which in-turn effects $\varepsilon(z)$) and the area under the curve (integral constant affecting length reduction) are much less in the case of graded-index fibers compared to the case of step-index fibers. In this comparison, the area under the $G(r)$ curve for the step-index case is about 2.5 times larger than the area under the $G(r)$ curve for the graded index curve, indicating that a shorter device length could be used under the same linear taper profile. Here, we have calculated the integral in eqn.(7) for both the cases and compared them considering both the cases to be having a linear taper profile. Thus, the usage of graded index SMFs leads to a more adiabatic propagation, which reduces inter-modal coupling and retains modal purity. The modifications in geometric and material parameters of the structure translates into the mathematical quantities of $G(r)$ and the integral constant. This method is therefore generic and could be used for optimizing adiabaticity by tweaking different device parameters.

4. Practical Configurations

The optimized profile mathematically obtained and presented in Fig. 4 and Fig. 7 may not be amenable to easy fabrication due to rapid slopes in the beginning and towards the end of the device. In these regions, the mode coupling is low and the values of $G(r)$ are very small. In order to obtain the required value of ε_c, eqn.(6) requires large $\frac{dr}{dz}$. This may be modified to more practically realisable configurations with relative ease. As an example, we consider the three-core case and the optimal profile presented in Fig. 4. Initially the radius tapers rapidly, since the value of $G(r)$ is low due to non-interacting and well confined modes in the individual SMFs. Mathematically, this reflects in $G(r)$ and thus in $\varepsilon(z)$. To tailor the required optimal variation of $r(z)$, we need to appropriately reduce $\varepsilon(z)$ in the region of low $G(r)$. We begin by relaxing the constant ε condition. Instead we design $\varepsilon(z)$ suitably while limiting its maximum value to ensure adiabaticity. This affects the desired length of the device and the straight forward inverse variation given in eqn.(9), no longer holds. In Fig. 9 a tangent hyperbolic like variation ($\varepsilon'_{opt}(z)$) is considered to appropriately contain the rapid variation in $r_{opt}(z)$ at the untapered end. This affects the length of the device, which is then calculated using eqn.(7).

To compute the revised optimal taper profile, we simply consider the newly defined variation of $\varepsilon(z)$ in eqn.(6).The computed profile is plotted in Fig. 10. The most optimal $\varepsilon(z)$ would be a constant and any changes to that would result in compromising the device length or adiabaticity. In the example discussed, an initial slow variation of $\varepsilon(z)$ eventually leading on to the constant value of ε_c results in a larger device length. Similarly, the rapid variation at the tapered end is also contained by a suitably designed $\varepsilon''_{opt}(z)$ resulting in an optimal $r(z)$ given as $r''_{opt}(z)$ in Fig. 10. In both the cases we see a penalty of device length incurred. This could be compensated by a compromise in adiabaticity by suitably raising the value of $\varepsilon(z)$, if possible. For example, in the 3-core device

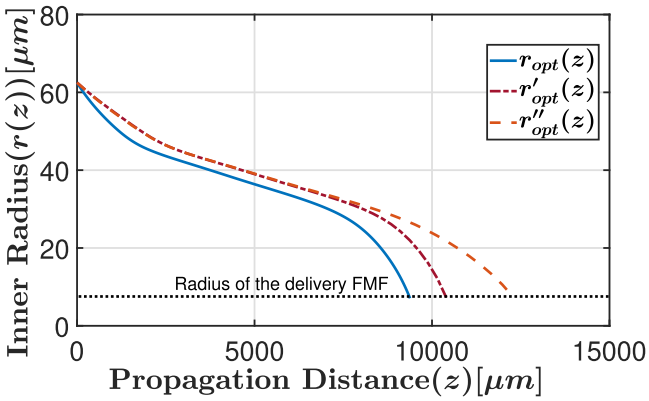

Fig. 10. Optimized taper profiles $r'_{opt}(z)$ and $r''_{opt}(z)$ corresponding to $\varepsilon'_{opt}(z)$ and $\varepsilon''_{opt}(z)$ show that tailoring of $\varepsilon_{opt}(z)$ can moderate the rapid variations in $r_{opt}(z)$ with a penalty on the device length.

example, the maximum value of ε_c is about 0.04 which is still very small compared to unity. In this case, one could increase the maximum value of ε_c to reduce the device length. However, in the 6-core device, ε_c is already close to unity and hence there is not much room for further relaxation. This is due to the limitation of the device in terms of the fiber sizes, indices, index profile, etc. and may require redesign as discussed in [43].

This simple procedure to appropriately tweak $\varepsilon(z)$ would be extremely useful in designing optimally quasi-adiabatic and experimentally feasible taper profiles.

5. Summary and Conclusion

Adiabaticity is critical for the performance of photonic lanterns and it is affected by various construction parameters of the device. We have presented a procedure to optimize adiabaticity by tailoring the taper profile. Optimization can improve the device adiabaticity or reduce the device length or both. The method is based on a shortcuts-to-adiabaticity (STA) protocol and it has been used to optimize the adiabatic taper profile in all-fiber photonic lanterns. The effect of cross-sectional device parameters on adiabaticity was also discussed. The adiabaticity criterion is used to the quantify inter-modal coupling which shows an inverse dependence on the device length. The protocol is successfully applied to reported three-core and six-core photonic lantern devices. Taper profiles with improved adiabaticity and shorter device lengths have been obtained. This method may be extended to optimize the design parameters of other adiabatic photonic devices. The method promises to be an invaluable tool towards miniaturization in photonics.

Acknowledgment

The authors thank *Baadal*, cloud computing facility IIT Delhi and *PADUM*, IIT Delhi supercomputer facility for computational resources.

Disclosures

The authors declare no conflicts of interest.

References

[1] M. Born and V. Fock, “Proof of the adiabatic theorem (in German),” *Zeitschrift Für Physik*, vol. 51, no. 3-4, pp. 165–180, 1928.

[2] Howard M. Wiseman and Gerard J. Milburn, *Quantum Measurement and Control*. Cambridge, U.K.: Cambridge Univ. Press, 2009.
[3] Z. Leghtas, A. Sarlette, and P. Rouchon, "Adiabatic passage and ensemble control of quantum systems," *J. Phys. B: Atomic, Mol. Opt. Phys.*, vol. 44, no. 15, 2011, Art. no. 154017.
[4] J. E. Avron, R. Seiler, and L. G. Yaffe, "Adiabatic theorems and applications to the quantum Hall effect," *Commun. Math. Phys.*, vol. 110, no. 1, pp. 33–49, Mar. 1987. [Online]. Available: https://doi.org/10.1007%2Fbf01209015
[5] M. V. Berry, "Transitionless quantum driving," *J. Phys. A: Math. Theor.*, vol. 42, no. 36, 2009, Art. no. 365303.
[6] A. C. Santos and M. S. Sarandy, "Superadiabatic controlled evolutions and universal quantum computation," *Sci. Rep.*, vol. 5, no. 1, pp. 1–10, 2015.
[7] Marlan O. Scully and M. Suhail Zubairy. *Quantum Optics*. Cambridge, U.K.: Cambridge Univ. Press, 1997.
[8] P. Li Kam Wa, N. Mason, J. Roberts, P. Robson, and J. Sitch, "All optical multiple-quantum-well waveguide switch," *Electron. Lett.*, vol. 21, no. 1, pp. 26–28, 1985.
[9] J. Love, "Spot size, adiabaticity and diffraction in tapered fibres," *Electron. Lett.*, vol. 23, no. 19, pp. 993–994, 1987.
[10] J. Love, W. Henry, W. Stewart, R. Black, S. Lacroix, and F. Gonthier, "Tapered single-mode fibres and devices. Part 1: Adiabaticity criteria," *IEE Proc. J. (Optoelectronics)*, vol. 138, no. 5, pp. 343–354, Oct. 1991.
[11] W. Walasik, N. Chandra, B. Midya, L. Feng, and N. M. Litchinitser, "Mode-sorter design using continuous supersymmetric transformation," *Opt. Exp.*, vol. 27, no. 16, pp. 22429–22438, 2019.
[12] J. Love, R. Vance, and A. Joblin, "Asymmetric, adiabatic multipronged planar splitters," *Opt. Quantum Electron.*, vol. 28, no. 4, pp. 353–369, 1996.
[13] S. Yerolatsitis, I. Gris-Sánchez, and T. Birks, "Adiabatically-tapered fiber mode multiplexers," *Opt. Exp.*, vol. 22, no. 1, pp. 608–617, 2014.
[14] S. G. Leon-Saval, T. Birks, J. Bland-Hawthorn, and M. Englund, "Multimode fiber devices with single-mode performance," *Opt. Lett.*, vol. 30, no. 19, pp. 2545–2547, 2005.
[15] A. Velazquez-Benitez *et al.*, "Six mode selective fiber optic spatial multiplexer," *Opt. Lett.*, vol. 40, no. 8, pp. 1663–1666, 2015.
[16] T. Morioka, "New generation optical infrastructure technologies: "EXAT initiative" towards 2020 and beyond," in *Proc. 14th OptoElectronics Commun. Conf.*, 2009, pp. 1–2.
[17] Y. Li *et al.*, "Design of OAM mode-selective photonic lanterns for mode division multiplexing systems," in *Proc. 24th OptoElectronics Commun. Conf. Int. Conf. Photon. Switching Comput.*, 2019, pp. 1–3.
[18] S. Sunder and A. Sharma, "Optimizing quasi-adiabaticity and its application in photonic lantern devices," in *Next-Generation Optical Communication: Components, Sub-Systems, and Systems IX*, vol. 11309. International Society for Optics and Photonics, 2020, Art. no. 1130906.
[19] S. G. Leon-Saval, A. Argyros, and J. Bland-Hawthorn, "Photonic lanterns," *Nanophotonics*, vol. 2, no. 5-6, pp. 429–440, 2013.
[20] S. Sunder and A. Sharma, "Generation of orbital angular momentum modes using photonic lanterns," in *Proc. Workshop Recent Adv. Photon.*, 2019, pp. 1–3.
[21] T. A. Birks, I. Gris-Sánchez, S. Yerolatsitis, S. Leon-Saval, and R. R. Thomson, "The photonic lantern," *Adv. Opt. Photon.*, vol. 7, no. 2, pp. 107–167, 2015.
[22] S. G. Johnson, P. Bienstman, M. Skorobogatiy, M. Ibanescu, E. Lidorikis, and J. Joannopoulos, "Adiabatic theorem and continuous coupled-mode theory for efficient taper transitions in photonic crystals," *Phys. Rev. E*, vol. 66, no. 6, 2002, Art. no. 066608.
[23] X. Sun, H.-C. Liu, and A. Yariv, "Adiabaticity criterion and the shortest adiabatic mode transformer in a coupled-waveguide system," *Opt. Lett.*, vol. 34, no. 3, pp. 280–282, 2009.
[24] R. MacKenzie, A. Morin-Duchesne, H. Paquette, and J. Pinel, "Validity of the adiabatic approximation in quantum mechanics," *Phys. Rev.*, vol. 76, no. 4, 2007, Art. no. 044102.
[25] D. Loss, H. Schoeller, and P. M. Goldbart, "Observing the berry phase in diffusive conductors: Necessary conditions for adiabaticity," *Phys. Rev. B*, vol. 59, no. 20, 1999, Art. no. 13328.
[26] L. C. Venuti, T. Albash, D. A. Lidar, and P. Zanardi, "Adiabaticity in open quantum systems," *Phys. Rev.*, vol. 93, no. 3, 2016, Art. no. 032118.
[27] S. Teufel. *Adiabatic Perturbation Theory in Quantum Dynamics*. Berlin, Germany: Springer, 2003.
[28] R. Black, S. Lacroix, F. Gonthier, and J. Love, "Tapered single-mode fibres and devices. II. Experimental and theoretical quantification," *IEE Proc. J-Optoelectron.*, vol. 138, no. 5, pp. 355–364, 1991.
[29] R. Kenny, T. Birks, and K. Oakley, "Control of optical fibre taper shape," *Electron. Lett.*, vol. 27, no. 18, pp. 1654–1656, 1991.
[30] S. Martínez-Garaot, J. G. Muga, and S.-Y. Tseng, "Shortcuts to adiabaticity in optical waveguides using fast quasiadiabatic dynamics," *Opt. Exp.*, vol. 25, no. 1, pp. 159–167, 2017.
[31] E. Torrontegui *et al.*, "Shortcuts to Adiabaticity," *Adv. Atomic, Mol., Opt. Phys.*, vol. 62, pp. 117–169, 2013.
[32] L. Shen *et al.*, "Highly mode selective 3-mode photonic lantern through geometric optimization," in *Proc. Opt. Fiber Commun. Conf. Expo.*, 2018, pp. 1–3.
[33] S. Sunder and A. Sharma, "Adiabatic propagation algorithm for photonic lanterns," *Opt. Fiber Technol.*, vol. 57, 2020, Art. no. 102219.
[34] A. Sharma and S. Sunder, "Modal and propagation studies of photonic lanterns," in *Proc. URSI Asia-Pacific Radio Sci. Conf.*, 2019, pp. 1–1.
[35] N. K. Fontaine, R. Ryf, J. Bland-Hawthorn, and S. G. Leon-Saval, "Geometric requirements for photonic lanterns in space division multiplexing," *Opt. Exp.*, vol. 20, no. 24, pp. 27123–27132, 2012.
[36] B. Rahman and A. Agrawal, *Finite Element Modeling Methods for Photonics*. Norwood, MA, USA: Artech, 2013.
[37] D. Heatley, G. Vitrant, and A. Kevorkian, "Simple finite-difference algorithm for calculating waveguide modes," *Opt. Quantum Electron.*, vol. 26, no. 3, pp. S 151–S163, 1994.
[38] S. Banerjee and A. Sharma, "Propagation characteristics of optical waveguiding structures by direct solution of the helmholtz equation for total fields," *JOSA A*, vol. 6, no. 12, pp. 1884–1894, 1989.

[39] R. Kumar and A. Sharma, "Absorbing boundary condition (ABC) and perfectly matched layer (PML) in numerical beam propagation: A comparison," *Opt. Quantum Electron.*, vol. 51, no. 2, pp. 1–13, 2019.
[40] A. Velazquez-Benitez *et al.*, "Six spatial modes photonic lanterns," in *Proc. Opt. Fiber Commun. Conf. Opt. Soc. Amer.*, 2015, pp. W 3B–3.
[41] S. Yerolatsitis and T. Birks, "Six-mode photonic lantern multiplexer made from reduced-cladding fibres," in *Proc. Eur. Conf. Opt. Commun.*, 2015, pp. 1–3.
[42] A. Velazquez-Benitez *et al.*, "Six mode selective fiber optic spatial multiplexer," *Opt. Lett.*, vol. 40, no. 8, pp. 1663–1666, 2015.
[43] X. Sai *et al.*, "Design of elliptical-core mode-selective photonic lanterns with six modes for MIMO-free mode division multiplexing systems," *Opt. Lett.*, vol. 42, no. 21, pp. 4355–4358, 2017.
[44] B. Huang *et al.*, "Mode-group-selective photonic lantern using graded-index multimode fibers," in *Proc. Opt. Fiber Commun. Conf. Opt. Soc. Amer.*, 2015, pp. W 2A–9.
[45] Y. Kokubun, T. Watanabe, S. Miura, and R. Kawata, "Proposal of MIMO-free mode divison multiplexed transmission using true eigenmodes," in *Proc. IEEE Photon. Soc. Summer Topical Meeting Ser.*, 2016, pp. 234–235.
[46] P. J. Winzer and G. J. Foschini, "MIMO capacities and outage probabilities in spatially multiplexed optical transport systems," *Opt. Exp.*, vol. 19, no. 17, pp. 16 680–16 696, 2011.